

# The Effect of Ferrite Embrittlement in Duplex Steel on Fatigue Crack Propagation from the Low (LCF) to the Very High Cycle Fatigue (VHCF) Regime

María Cecilia Marinelli<sup>1,3,a</sup>, Alexander Giertler<sup>1,b</sup>, Jitendra Kumar Sahu<sup>2,c</sup>,  
Silvina Hereñú<sup>3,d</sup>, Iris Alvarez-Armas<sup>3,e</sup> and Ulrich Krupp<sup>1,f</sup>

<sup>1</sup> Faculty of Engineering and Computer Science, University of Applied Sciences Osnabrück,  
Germany

<sup>2</sup> CSIR-National Metallurgical Laboratory, Jamshedpur, India

<sup>3</sup> Instituto de Física Rosario, Universidad Nacional de Rosario, Argentina

<sup>a</sup> m.marinelli@hs-osnabrueck.de, <sup>b</sup> a.giertler@hs-osnabrueck.de, <sup>c</sup> jksahu@nmlindia.org,

<sup>d</sup> herenu@ifir-conicet.gov.ar, <sup>e</sup> alvarez@ifir-conicet.gov.ar, <sup>f</sup> u.krupp@hs-osnabrueck.de

**Keywords:** duplex stainless steels, 475° embrittlement, fatigue crack initiation and propagation

**Abstract.** The excellent combination of mechanical properties and corrosion resistance of duplex stainless steel is obtained from balanced amount of ferrite and austenite in the microstructure. However, this grade of steel embrittles when exposed in the temperature range of 280–500°C limiting its application to temperatures below 280°C. To study the effect of embrittlement on fatigue behavior at high strain ranges, plastic-strain- controlled LCF test and at low strain ranges, stress-controlled HCF/VHCF tests were conducted on 1.4462 duplex steel and accompanied by SEM analysis in combination with EBSD. Extensive TEM was done to study the micromechanism of fatigue crack initiation and propagation across the strain ranges.

## Introduction

The problem to apply ferritic stainless steel at elevated temperature is due to 475°C embrittlement and it is well known [1-4]. The spinodal decomposition of the ferritic phase to chromium-rich phase ( $\alpha'$ ) and iron-rich phase ( $\alpha$ ) in the temperature range of 280–500°C due to the presence of a miscibility gap in iron–chromium binary alloy system embrittles the microstructure. Since this problem was inherent to ferritic microstructure research emphasis on the embrittlement problem in this temperature range was mostly confined to solely binary iron–chromium alloys and, in some cases, commercial grades of ferritic stainless steels [1-4]. Duplex stainless steels (DSSs), on the other hand, contain both ferrite and austenite in varying proportions in the microstructure and is undergoing continuous evolution to newer grades primarily based on adjusting the chemical composition and processing route. The main drawback of the embrittlement is that it modifies the tensile and fracture behaviour of this steel. Many applications imply cyclic loading and thus the prediction of the fatigue life or the residual fatigue life as well as the knowledge of fatigue limit is essential. Fatigue limit is based on the assumption that below a certain stress value no cycle-dependent damage occurs. Krupp et al. [5] have found that standard DSS exhibits a technical fatigue limit up to  $N = 10^8$  cycles since phase boundaries were identified as effective barriers against slip

transfer. In the embrittled material, the information about cyclic behavior is very scarce. Recently, it was reported that fatigue life of a standard DSS is longer in the aged condition at lower strain amplitudes as compared to the non-aged condition, it becomes similar at intermediate strain amplitude and it is shorter at higher strain amplitude [6].

Evolution of surface roughness, subsequent nucleation and growth of short crack in DSS by cyclic loading is strongly influenced by the microstructural parameters, i.e., grain size, grain orientation, grain and phase boundary geometry and precipitates. The crack initiation and growth in individual grains in DSS depend on the orientation, inherent strength and toughness properties of neighboring grains and it is very important to know and understand how these factors determines fatigue damage evolution. Alvarez-Armas et al.[7] have reported that during LCF in the embrittled DSS microcracks initiate with a very high density firstly in the embrittled ferrite and propagate along slip markings in the austenite, while in high cycle fatigue (HCF) crack nucleation is either in  $\alpha$ - $\alpha$  boundary or in  $\alpha$ - $\gamma$  boundary in the intersection of slip bands in the austenite. On the other hand, Llanes et al.[8] have reported for an embrittled standard DSS, pronounced slip bands in the austenite, which develop marked extrusions where cracks initiate, while the aged ferrite hardly shows only traces of damage. HCF and VHCF studies on austenitic ferritic duplex steel specimens in two different heat treatment conditions have revealed that even beyond  $10^8$  cycles local plasticity causes surface modifications in form of pronounced slip bands that are extending with an increasing number of cycles [9].

Therefore, the gray area remains in the change of deformation mechanisms due to 475°C embrittlement of DSS in the ferritic and austenitic phase. In the present paper, the study of the effect of the embrittlement on the fatigue limit and cracks propagation is carried out from scanning electron microscopy observations (SEM) in combination with electron backscattered diffraction (EBSD). Moreover, the dislocation structure developed was analyzed and correlated with the formation and propagation of microcracks.

### Experimental procedure

The behavior of microstructurally short fatigue cracks was studied in an austeno-ferritic duplex stainless steel with the German designation DIN 1.4462. The chemical composition of the material is: C: 0.02; Cr: 21.9; Ni: 5.6; Mo: 3.1; Mn: 1.8; N: 0.19; P: 0.023; S: 0.002; Fe balance. After a 4 hours homogenization heat treatment at 1250°C followed by slow-cooling to 1050°C and quenching in water, the microstructure consists of approximately 50% austenite with a mean grain size of 30  $\mu\text{m}$  embedded in 50% ferrite with a mean grain size of 27  $\mu\text{m}$ , Fig 1. Finally, the material was aged at 475°C for 100hrs, resulting in Vickers hardness values of (HV 0.05, 10 sec) 254 HV in the austenite and 465 HV in the ferrite, respectively.

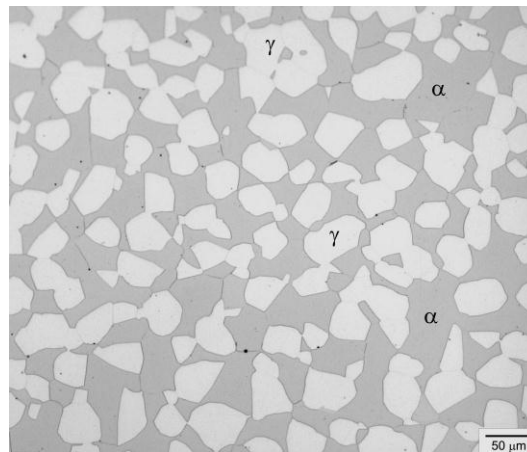


Fig. 1. Optical micrograph on the two-phase structure of 1.4462 DSS after the homogenization heat treatment.

Cylindrical shallow notched specimens for LCF and HCF were machined. The notch focuses the fatigue damage in the zone of observation. Prior to testing, the specimens were ground and electro-polished to eliminate any roughness. The central part of the notch was monitored during the test using a portable optical microscope in combination with a CCD camera.

The tests for LCF were carried out under strain control with a fully reversed triangular wave at a constant total plastic-strain range of 0.3% and a total strain rate of  $2 \times 10^{-3} \text{ s}^{-1}$ . Push-pull fatigue tests were carried out at room temperature under stress control,  $\Delta\sigma/2 = 350 \text{ MPa}$ , stress ratio  $R = -1$  and frequency  $f = 5 \text{ Hz}$ . The specimens were analyzed by means of analytical SEM (Zeiss Auriga) in combination with automated EBSD and transmission electron microscopy (PHILIPS EM 300, 100KV).

## Experimental Results

Rotating bending fatigue tests were carried out to study the effect of the embrittling heat treatment on the fatigue limit of the duplex steel. The results as shown in Fig. 2a, have revealed that the embrittled condition increase the fatigue life compared with the as-received condition during HCF. However, during LCF the fatigue life becomes similar or shorter depending on the strain amplitude range (Fig 2b).

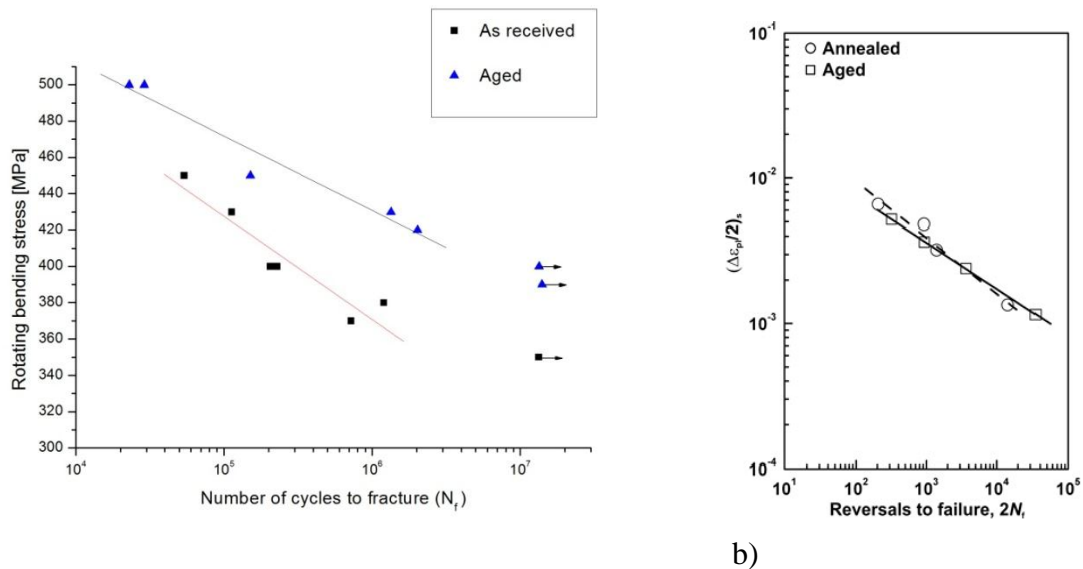


Fig. 2. a) S/N (Wöhler) diagram of the duplex steel 1.4462 for rotating bending in the as-received and in the embrittled condition; b) Plastic strain amplitude in saturation or mid life versus reversals to failure [6].

On examining the specimen surface during the cycling tests, different features were observed due to the cyclic plastic deformation process:

**Low Cycle Fatigue.** In a previous paper, the microcracks during LCF [7] were carefully characterized. The result of these investigations showed that microcracks nucleate either in the  $\alpha$ - $\alpha$  boundary or on slip planes with high Schmid factor (SF) in the ferrite phase. The propagation in the short crack regime involves either single-slip with the highest SF or an alternating double-slip mechanism [10]. In the present investigation, Fig. 3a shows typical microcrack growth behavior during this regime. It initiates at the  $\alpha$ - $\alpha$  boundary and propagates in the neighboring austenitic grains with a crack propagation rate almost constant (Fig. 3b). In grain #1 the crack starts to grow on a single-slip plane with  $SF = 0.38$  and after few cycles, an additional slip system is activated

$(\bar{1}\bar{1}1)[101]$  with the highest SF= 0.47 resulting in crack propagation on multiple slip bands. In the austenite grain #2 the crack grows by operating two slip systems  $(\bar{1}\bar{1}1)[011]$  and  $(111)[0\bar{1}\bar{1}]$  slip system with SF= 0.49 and SF= 0.48, respectively. It is interesting to note that after several cycles the crack returns to single-slip propagation on the  $(\bar{1}\bar{1}1)$  plane with the highest SF.

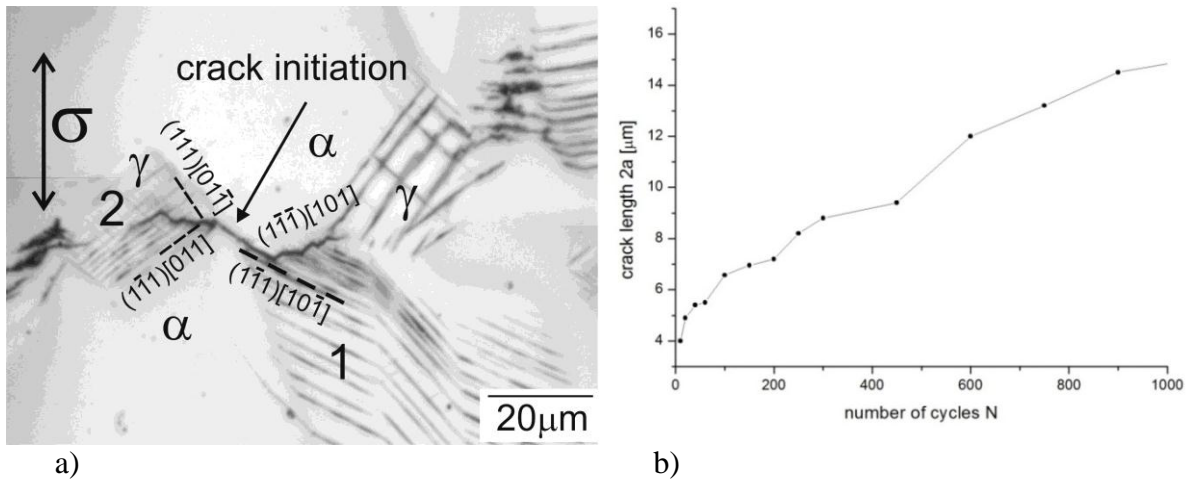


Fig. 3. a) CCD micrograph showing the surface damage after LCF. The traces of the slip planes and SF calculated according to the EBSD results are included; b) crack length as a function of number of cycles.

**High Cycle Fatigue.** During HCF in the embrittled DSS, the first slip markings appear mostly in the austenitic phase before reaching the first 1000 cycles. As cycling proceeds, slip lines in the austenitic phase intensify and some propagate into the neighboring ferritic grains or remain arrested at boundaries. As was already reported by the authors [7], microcrack behavior mainly follows two different situations: i) nucleation at the  $\alpha$ - $\alpha$  boundary and propagation along the grain boundary up to the next  $\alpha$ - $\gamma$  boundary; ii) nucleation at the  $\alpha$ - $\gamma$  boundary and propagation in the  $\alpha$ -grain up to the next barrier. However, microcracks nucleated in slip markings in austenite were also observed but less frequently. Fig. 4a shows a microcrack that initiates at the  $\alpha$ - $\gamma$  boundary and propagates on the left-hand crack tip, along the  $(\bar{1}\bar{1}2)[1\bar{1}1]$  system with SF= 0.46 in a ferritic grain, while on the right-hand crack tip the crack grows in the austenitic grain (black dashed line) by double slip on  $(\bar{1}\bar{1}1)[011]$  and  $(\bar{1}\bar{1}1)[110]$  systems with the highest Schmid factor, SF= 0.45 and SF= 0.41, respectively. As is shown in Fig. 4a, the direction of subsequent crack propagation can be represented by the vector addition of the displacements along the two slip systems. The corresponding crack length as a function of the number of cycles for this example of microcrack propagation is represented in Fig. 4b. According to microcrack growth behavior, phase boundaries represent an efficient barrier to crack propagation. From the previous results, it seems that the barrier effect of the phase boundaries is generally higher than the barrier effect of the ordinary  $\alpha$ - $\alpha$  and  $\gamma$ - $\gamma$  grain boundaries, irrespective of the angles between possible slip systems in the adjacent grains [10].

Fig. 5a shows the cross stitch- dislocation structure in the embrittled ferrite. It is interesting to note that where the pile-ups in the austenite impinge the phase boundary, a high stress concentration zones is created in the ferrite (Fig. 5b).

Comparing with the as-received DSS in the same conditions of cycling test, the cyclic plastic activity begins, after few cycles in the austenitic phase. As cycling proceeds, slip lines intensify and finally most of these propagate into the ferrite. It is interesting to note that the concentration of

stresses in the ferrite increases and slip markings intensify and turn into coarse bands that could be remain arrested at the grain boundary (Fig. 6a). As revealed by TEM observation, the microstructure in the austenite consists of planar arrangement of dislocation pile-ups in two slip systems and the dislocation structure in ferrite consist of loops patches (Fig. 6b). Therefore, in the as-received condition plastic deformation involves both phases. The Fig. 6b shows bands in austenite propagating on a ferritic grain. In this case there is not high stress concentration at the grain boundary and the dislocations easily pass through it.

During VHCF the formation of pronounced slip bands in austenite was observed, which piled up at the  $\gamma$ - $\alpha$  phase boundary as shown in Fig. 7.

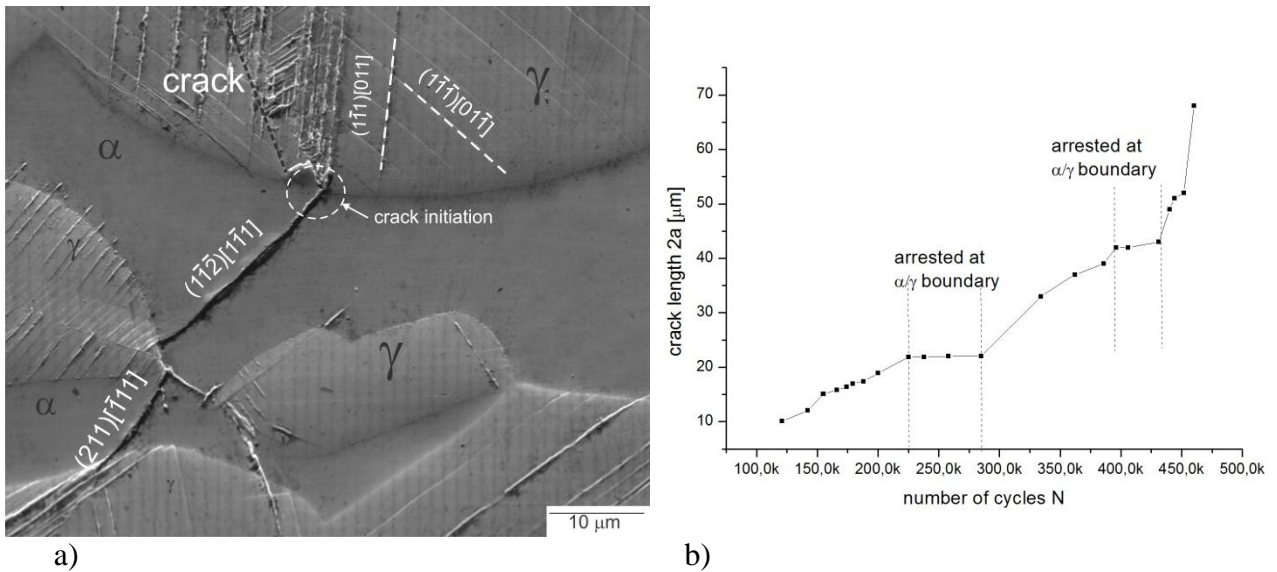


Fig. 4. a) Scanning electron micrograph showing the crack path in HCF at  $\Delta\sigma/2= 350$  MPa; b) crack length vs. the number of cycles.

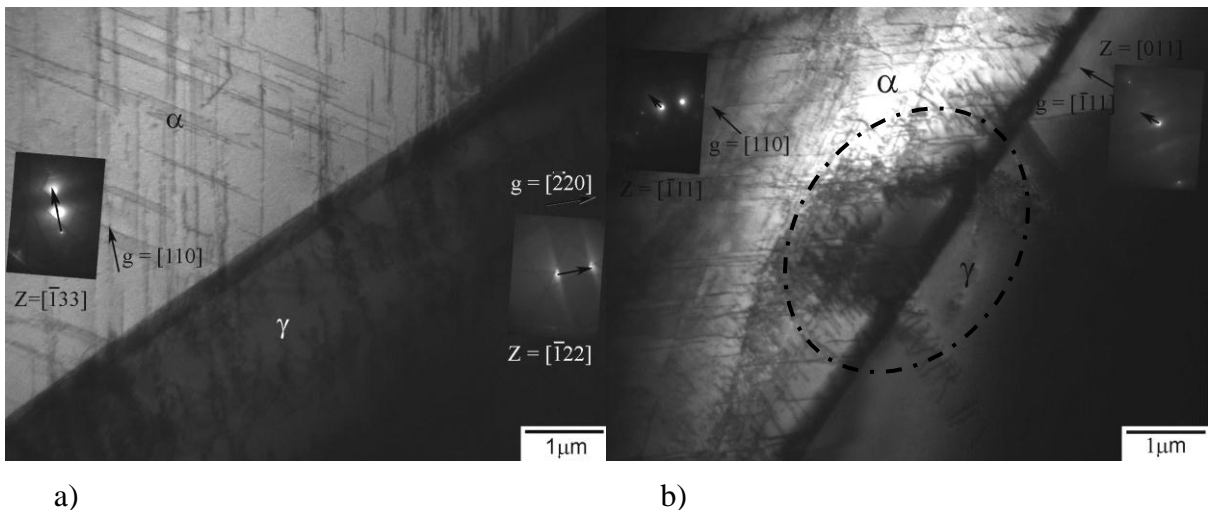


Fig. 5. a) Cross stitch dislocation structure in ferrite; b) high stress concentration zones due to pile-ups of dislocations at grain boundary.

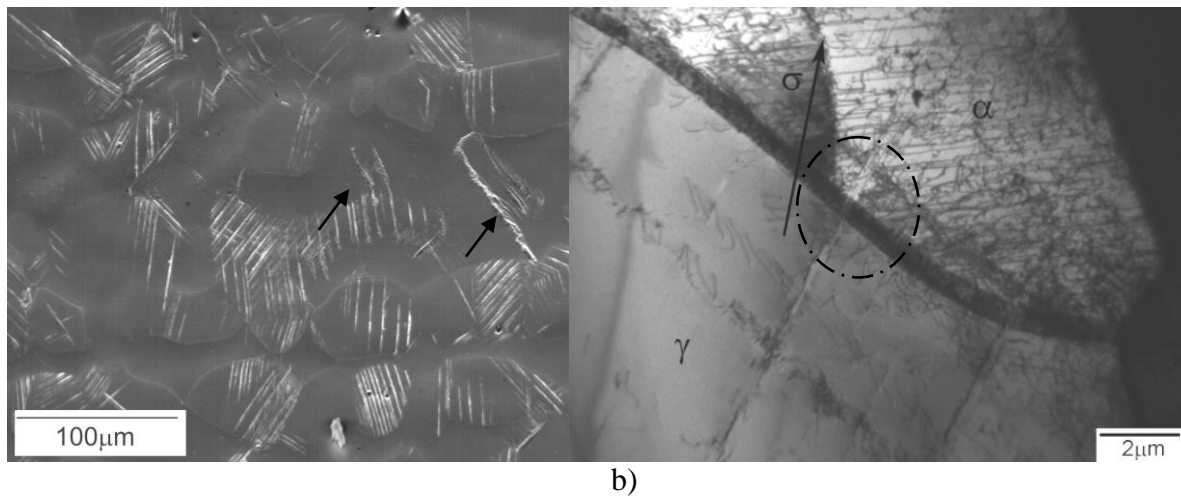


Fig. 6. a) Cyclic plastic activity in as-received DSS during HCF; b) dislocation pile-ups crossing a phase boundary.

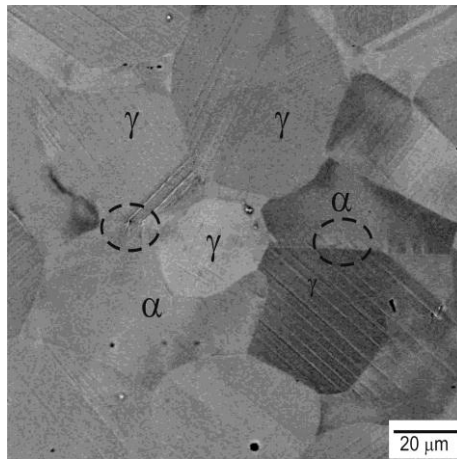


Fig.7. Slip bands in austenite, which piled up at the  $\gamma$ - $\alpha$  phase boundary during VHCF, in as-received DSS.

## Discussion

According to the rotating bending test on specimens of DSS, the results have revealed that the embrittled condition increase the fatigue life compared with the as-received condition during HCF and the situation is reversed in LCF. This fact was reported by Sahu et al. [6] in cycling fatigue tests conducted at different constant strain amplitudes for the annealed and the aged conditions. They established that the fatigue resistance of the material converges with increase in  $\Delta\epsilon/2$  values as a result of rapid cyclic softening of the ferritic phase in the aged condition. This cyclic softening of the ferrite, according to [11] could be related to the formation of microbands develop parallel to the most favorable slip planes [7]. Hereñú et al. [11] studied these bands and showed that they form as a consequence of a loss of embrittlement during cycling, i.e., the restoration of the ductility along narrow regions parallel to the traces of the ferrite planes with the highest SF. That is along the most favorable slip planes. Therefore, these areas can be considered as ribbons of soft  $\alpha$ -phase immersed in a matrix of hard  $\alpha'$  phase.

Llanes et al.[8] observed, in UNS S31803 aged at 475°C for 200h, that the high cycle fatigue strength is strongly affected by the crack nucleation stage in the softer phase, i.e., austenite.

However, in the present study the cracks during HCF initiate mainly at the  $\alpha$ - $\gamma$  boundary. Taisne et al. [12] observed in a recent study on the role of interfaces in fatigue deformation mechanism in DSS bicrystal, that phase boundary geometry and elasticity affects the dislocation transmission process. Moreover, Marinelli et al. [13, 14] studied Kurjumov–Sachs crystallographic orientation relations between austenite (fcc) and ferrite (bcc) in DSS. They observed that the efficiency of the coupling between phases seems to play an important role in the crack formation process. In the current study, the TEM observation has shown that in HCF the ferrite is practically inactive. However, where the pile-ups in the austenite impinge the phase boundary, stress concentration zones are created in the ferrite. This fact has been attributed to a consequence of the higher cyclic yield stress of the embrittled ferrite, which might require a higher applied stress for plastic deformation leaving the austenite as the only phase that sustains plastic strain. However, once the capacity of the austenite grain to plastically deform is reached, the pile-ups generate strong stress concentration zones at the phase boundary capable to allow the nucleation of microcracks and the activation of slip systems in the adjoining ferrite. On the other hand, in the as-received DSS during HCF the pile-ups can more easily cross the phase boundary continuing along of slip plane in the adjoining softer ferrite grain. In this case, the deformation is developed in both phases. However, the concentration of stresses in the ferrite increases with cycling and slip markings intensify and turn into coarse bands, which preferably become sites of crack nucleation. Zielinski et al. [15] studied the evolution of dislocation structure in an annealed DSS by in-situ TEM straining experiments and reported that the evolution of dislocation structure during straining was dependent on the orientation relationship between the two phases. In the case of special orientation relationships, the slip markings in the ferrite, produced by the dislocations emitted from the boundary, indicate the compatibility of easy slip systems in the two phases, which favors a strong localization of strain. In the case of random orientation relationships, the incompatibility of the easy slip systems in austenite and ferrite results in the cross slip of the dislocations emitted from the boundary into the ferrite grains leading to multiplication and the formation of dislocation loops and debris. They attributed the high flow stress of DSS to the particular slip transfer mechanism related to the random orientation relationships between the austenite and ferrite.

Consequently, the aged condition in HCF regime retards plastic deformation in the ferrite, strengthens the phase boundaries and, therefore, prevents the early crack propagation. On the other hand, during LCF the embrittled ferrite presents plastic deformation forming microbands that preparing a path in which the crack grows.

## **Summary**

On the basis of an experimental study of the damage evolution during low and high cycle fatigue behavior in an embrittled duplex stainless steel (DSS) (DIN 1.4462), the effect of the embrittlement on the fatigue limit and crack propagation was studied. It was observed that the embrittled ferritic phase increase the fatigue life in HCF regime, strengthening the phase boundaries. In this regime the plastic deformation is limited to austenite and the microcracks initiate mostly at  $\alpha$ - $\gamma$  boundaries and then propagate along slip markings formed successively in the austenitic and ferritic grains. In the as-received DSS the plastic deformation is present in both phases and the cracks initiate mostly along slip bands in the ferrite. On the other hand, during VHCF the formation of pronounced slip bands in austenite was observed.

During LCF the embrittled ferrite develops microbands, which seems to be the most favorable dislocation structure for microcrack initiation. The crack propagation can operate either by single-slip or double-slip. Additionally, it was found that a crack, which has grown in double slip, can change to the single slip mechanism even in the same grain.

## References

- [1] H.D. Solomon, L.M. Levinson: *Acta Metallurgica*. Vol. 26 (3) (1978), p. 429.
- [2] D. Chandra, L.H. Schwartz: *Metallurgical Transactions*. Vol. 2 (1971), p. 511.
- [3] P.J. Grobner: *Metallurgical Transactions*. Vol. 4 (1973), p. 251.
- [4] M.B. Cortie, H. Pollak: *Materials Science and Engineering A*. Vol.199 (1995), p 153.
- [5] U. Krupp, H. Knobbe, H.J. Christ, P. Köster, C.P. Fritzen: *Int J Fatigue*. Vol. 32, 6 (2010), p.914.
- [6] J. K. Sahu, R. N. Ghosh, H.J. Christ: *Fatigue Fract Engng Mater Struct*. Vol. 33 (2009), p.77
- [7] I. Alvarez-Armas, U. Krupp, M. Balbi, S. Hereñú, M.C. Marinelli, H. Knobbe: *Int J Fatigue*. Vol. 41(2012), p. 95.
- [8] L. Llanes, A. Mateo, P. Violan, J. Méndez, M. Anglada: *Materials Science and Engineering A* Vol. 234–236 (1997), p. 850.
- [9] U. Krupp, A. Giertler, M. C. Marinelli, H. Knobbe, H.J. Christ, P. Köster, C.P. Fritzen, S. Hereñú, I. Alvarez: *proceeding Fifth International Conference on Very High Cycle Fatigue*, edited by C. Berger and H.J. Christ, Berlin (2011), p.127
- [10] O. Düber, B. Künkler, U. Krupp, HJ. Christ, CP. Fritzen: *Int J Fatigue* Vol. 28 (2006), p. 983.
- [11] S. Hereñú, M. Sennour, M. Balbi, I. Alvarez-Armas, A. Thorel, AF Armas: *Mater Sci Eng A* Vol. A528 (2011), p. 7636.
- [12] Taisne, B. Decamps, L. Priester: *Composite Interfaces* Vol. 13 (1) (2006), p. 89.
- [13] Ma.C. Marinelli, A. El Bartali, J.W. Signorelli, P. Evrard, V. Aubin, I. Alvarez-Armas, S. Degallaix-Moreuil: *Mater Sci Eng A* Vol. 509 (2009), p. 81.
- [14] M.C. Marinelli, M.G. Moscato, J.W. Signorelli, A. El Bartali, I. Alvarez-Armas: *Key Engineering Materials* Vol. 465 (2011), p. 415.
- [15] W. Zielinski, W. Witnicki, M. Barstch, U. Messerschmidt: *Material Chemistry and Physics* Vol. 81 (2–3) (2003), p. 476.